



Published in final edited form as:

Dev Biol. 2016 February 15; 410(2): 150–163. doi:10.1016/j.ydbio.2015.12.027.

FGFR and PTEN signaling interact during lens development to regulate cell survival

Blake R. Chaffee^{*,†}, Thanh V. Hoang^{*,†}, Melissa R. Leonard^{*}, Devin G. Bruney^{*}, Brad D. Wagner^{*}, Joseph Richard Dowd^{*}, Gustavo Leone[§], Michael C. Ostrowski[§], and Michael L. Robinson^{*}

^{*}Department of Biology, Cell Molecular and Structural Biology Graduate Program, Miami University, Oxford, OH, USA

[§]Department of Molecular Virology, Immunology and Medical Genetics, Department of Molecular Genetics, The Comprehensive Cancer Center, The Ohio State University, Columbus, OH, USA

Abstract

Lens epithelial cells express many receptor tyrosine kinases (RTKs) that stimulate PI3K-AKT and RAS-RAF-MEK-ERK intracellular signaling pathways. These pathways ultimately activate the phosphorylation of key cellular transcription factors and other proteins that control proliferation, survival, metabolism, and differentiation in virtually all cells. Among RTKs in the lens, only stimulation of fibroblast growth factor receptors (FGFRs) elicits a lens epithelial cell to fiber cell differentiation response in mammals. Moreover, although the lens expresses three different *Fgfr* genes, the isolated removal of *Fgfr2* at the lens placode stage inhibits both lens cell survival and fiber cell differentiation. Phosphatase and tensin homolog (PTEN), commonly known as a tumor suppressor, inhibits ERK and AKT activation and initiates both apoptotic pathways, and cell cycle arrest. Here, we show that the combined deletion of *Fgfr2* and *Pten* rescues the cell death phenotype associated with *Fgfr2* loss alone. Additionally, *Pten* removal increased AKT and ERK activation, above the levels of controls, in the presence or absence of *Fgfr2*. However, isolated deletion of *Pten* failed to stimulate ectopic fiber cell differentiation, and the combined deletion of *Pten* and *Fgfr2* failed to restore differentiation-specific Aquaporin0 and DnaseII β expression in the lens fiber cells.

Keywords

Lens; FGF Receptor; PTEN; Differentiation; Survival

Corresponding author: 258 Pearson Hall, Miami University, 700 East High Street, Oxford, OH 47056. Phone: 513-529-2353, FAX: 513-529-6900, Robinsm5@miamioh.edu.

[†]These authors contributed equally to this work.

Publisher's Disclaimer: This is a PDF file of an unedited manuscript that has been accepted for publication. As a service to our customers we are providing this early version of the manuscript. The manuscript will undergo copyediting, typesetting, and review of the resulting proof before it is published in its final citable form. Please note that during the production process errors may be discovered which could affect the content, and all legal disclaimers that apply to the journal pertain.

INTRODUCTION

The relative developmental simplicity of the ocular lens makes it an important model to study developmental mechanisms controlling cellular growth, survival, differentiation, and proliferation (Wormstone and Wride, 2011). Invaginations of surface ectoderm overlying the optic vesicles create bilateral lens vesicles during early mammalian development (reviewed in Robinson, 2014). Cells in the posterior hemisphere of the lens vesicle withdraw from the cell cycle, elongate, and turn on fiber cell specific genes as they differentiate into the primary fiber cells (reviewed in Bassnett and Beebe, 2004). The lens vesicle cells in the anterior hemisphere differentiate into the lens epithelium. Only lens epithelial cells proliferate, and as the lens matures, cell proliferation becomes increasingly restricted to the germinative zone, a narrow band of epithelial cells slightly anterior to the lens equator (Harding et al., 1971; McAvoy, 1978). Proliferation within the germinative zone displaces epithelial cells toward the equator where they differentiate into secondary fiber cells. Proliferation in the germinative zone and secondary fiber cell differentiation provide a constant source of new lens fibers throughout the mammalian lifespan.

Among the numerous receptor tyrosine kinases (RTKs) expressed in the developing lens, fibroblast growth factor receptors (FGFRs) play a unique and indispensable role in lens development (Garcia et al., 2011; Garcia et al., 2005; Madakashira et al., 2012; Robinson, 2006; Zhao et al., 2008). As with most RTKs, ligand (FGF) binding by FGFRs leads to downstream activation of intracellular phosphorylation cascades culminating in the activation, by phosphorylation, of ERK1/2 and AKT kinases. Activation of these kinases leads to many of the cellular responses associated with growth factor stimulation (Lemmon and Schlessinger, 2010). In lens explants, or cultured lens epithelial cells, AKT and/or ERK1/2 phosphorylation results in enhanced cell survival, growth, proliferation, and differentiation (Chandrasekhar and Sailaja, 2004a, b; Iyengar et al., 2006; Le and Musil, 2001a, b; Lovicu and McAvoy, 2001; Wang et al., 2009; Weber and Menko, 2006). However, eliminating or inhibiting FGFR signaling *in vivo* leads to decreased lens cell survival and differentiation without significantly altering cell proliferation (Chow et al., 1995 et al., 1995; Garcia et al., 2011; Garcia et al., 2005; Madakashira et al., 2012; Robinson et al., 1995; Stolen and Griep, 2000; Zhao et al., 2008).

The mouse lens specifically expresses three FGFR genes, *Fgfr1*, *Fgfr2* and *Fgfr3* (Hoang et al., 2014). Lenses lacking *Fgfr2* prior to the lens vesicle stage undergo degeneration marked by both apoptosis and differentiation defects, while simultaneously removing *Fgfr1* exacerbates this phenotype (Garcia et al., 2005; Garcia et al., 2011). Conditional deletion of *Fgfr1*, *Fgfr2* and *Fgfr3* receptors in the lens, subsequent to the lens vesicle stage, causes massive apoptosis and arrest of fiber cell differentiation (Zhao et al., 2008). Conversely, lenses that overexpress FGFs *in vivo* undergo ectopic fiber cell differentiation in the lens epithelium (Lovicu and Overbeek, 1998; Robinson et al., 1998; Robinson et al., 1995). FGFR activation requires heparan sulfate in a ternary complex with FGF. The loss of heparan sulfate synthesizing enzymes *Ndst1* and *Ndst2* causes lens cell apoptosis, reduced proliferation, and defective fiber cell differentiation (Qu et al., 2011). However, expression of a constitutively active *Ras* allele in these lenses increased ERK1/2 phosphorylation and reversed the *Ndst1/Ndst2* deficient phenotypes.

Since lens cells rely on FGFR signaling for survival, decoupling the apoptotic phenotype from the differentiation phenotype in lenses with compromised FGFR signaling remains a challenge. During normal development, FGFR signaling in the lens may primarily promote cell survival with defective differentiation in FGFR-deficient lenses resulting as a secondary response to apoptosis. AKT enhances cell survival by a variety of mechanisms, including inhibiting FOXO transcription factors and destabilizing the pro-apoptotic BAD/Bcl-X_L complex (reviewed in Zhang et al., 2011). FGFR stimulation activates phosphoinositide 3-kinase (PI3K) which converts the cell membrane lipid PtdIns (4,5)P₂, hereafter referred to as PIP₂, into PtdIns(3,4,5)P₃, hereafter referred to as PIP₃. PIP₃ then recruits AKT to the cell membrane where phosphorylation by mTORC2 and PDK1 activates AKT (Sarbasov et al., 2005). The tumor suppressor protein, Phosphatase and tensin homolog (PTEN), counteracts PI3K by dephosphorylating PIP₃ back to PIP₂, leading to reduced AKT activation. In addition to inhibiting AKT activation, PTEN acts as a tumor suppressor by inhibiting cell proliferation and promoting apoptotic pathways (Chung and Eng, 2005; Franke et al., 2003; Weng et al., 2001a).

Given the antagonism between PI3K and PTEN, we hypothesized that PTEN acts as an important negative regulator of FGFR activity during lens development. In particular, PTEN activity may drive lens cells toward apoptosis by exacerbating the presumably decreased PIP₃ levels in FGFR-deficient lens cells, which indirectly prevents the activation of AKT. Studies in both osteoprogenitor cells and keratinocytes reveal the importance of balancing FGFR and PTEN signaling. Deletion of *Fgfr2* rescues over-proliferation in osteoprogenitors caused by the loss of *Pten* (Guntur et al., 2011). Likewise, skin tumorigenesis resulting from *Pten* deletion requires *Fgfr2* (Hertzler-Schaefer et al., 2014). To specifically determine whether PTEN-signaling counter balances FGFR-signaling with respect to survival and/or differentiation in the lens, we used Cre-mediated recombination to facilitate the lens-specific removal of both *Pten* and *Fgfr2* during early lens development. We reasoned that the restoration of survival in FGFR-deficient lens cells would reveal survival-independent aspects of FGFR-mediated fiber cell differentiation.

Given the central importance of FGFR signaling in the development of many different tissues and organs (reviewed in Carter et al., 2015; Teven et al., 2014), it comes as no surprise that aberrant FGFR signaling causes numerous developmental disorders and drives the pathogenesis of many human cancers (reviewed in Ahmad et al., 2012; Katoh and Nakagama, 2014; Wesche et al., 2011). Often, the same mutations that give rise to developmental disorders in the germline lead to specific cancers in somatic tissues. Likewise, *PTEN* mutations drive the genesis and malignancy of several human tumors (reviewed in Mester and Eng, 2013). Revealing how FGFR and PTEN signaling interact in the context of lens development may facilitate the discovery of new targets for therapeutic intervention to treat diseases or conditions caused by FGFR and/or PTEN dysfunction.

MATERIALS AND METHODS

Mice

Mice were used in accordance to the ARVO statement for the Use of Animals in Ophthalmic and Visual Research with approval from the Miami University Institutional Animal Care

and Use Committee. Dr. Ruth Ashery-Padan at Tel Aviv University kindly provided the *Le-Cre* mice (Ashery-Padan et al., 2000). Mice engineered with loxP sites flanking exons 4 and 5 of *Pten* were previously described (Trimboli et al., 2009). Floxed *Fgfr2* mice (Yu et al., 2003) were obtained from Dr. David M. Ornitz from the Department of Molecular Biology and Pharmacology, Washington University Medical School.

Histology and Immunohistochemistry

The gestational age of experimental embryos was determined by vaginal plug detection, set at embryonic day 0.5 (E0.5). One hour prior to embryo collection, pregnant dams were injected intraperitoneally with (0.1 mg/g body weight) 5-bromo-2-deoxyuridine (BrdU) dissolved in phosphate-buffered saline (PBS). For paraffin wax-embedded sections, embryos were collected and fixed in 10% neutral buffered formalin (NBF). Standard protocols were used to process and embed tissues in paraffin wax before sectioning at 5 μ m. Immunohistochemistry staining identified protein localization on the paraffin lens sections. Briefly, the sections were subjected standard xylene washes to remove excess paraffin followed by tissue dehydration. The sections were antigen retrieved as described in (Zhao et al. 2008). Tissue sections were blocked using 10% normal horse or normal goat serum, dependent upon the antibody used. Primary antibodies for, BrdU and Aquaporin0 (ab6326, ab15077 respectively) were obtained from Abcam, Cambridge, MA, USA. The primary antibody for p27KIP1 (BD610241) was obtained from BD Biosciences, San Jose, CA, USA. The primary antibodies for β and γ -crystallin were kind gifts from Samuel Zigler at Johns Hopkins University School of Medicine. All primary and secondary antibodies were used at a 1:100 dilution, with the exception of β and γ -crystallin, which were used at a 1:250 dilution. Primary antibodies were detected using secondary antibodies attached to fluorescent probes (Alexa Fluor 488 goat anti-rabbit IgG, Alexa Fluor 546 goat anti-rat IgG, FITC for donkey antirabbit IgG, 711-095-152 and Cy3 for donkey anti-mouse IgG). Sections were counterstained with DAPI (H-1200, Vector Labs, Burlingame, CA, USA). Cells undergoing DNA degradation/apoptosis was detected using the In Situ Cell Death Detection Kit (TMR Red, Roche AppliedScience, 2156792). Photomicrographs were captured on a Zeiss 710 Laser Scanning Confocal System at the Center for Advanced Microscopy and Imaging at Miami University. Standard Hematoxylin and Eosin-stained sections were used to analyze the structure of the lens, and images were captured using a Nikon TI-80 microscope. The proliferation and apoptotic index represents a ratio of all the BrdU positive or TUNEL positive nuclei (respectively) over the total nuclei in the entire lens at E12.5. At E15.5 the proliferation and apoptotic index represents a ratio of BrdU or TUNEL positive nuclei in the lens epithelium over the total number of lens epithelial cells. The proliferation index and apoptotic index was calculated with respect to the whole lens at E12.5 due to the difficulty distinguishing fiber and epithelial cells in FGFR2-deficient lenses at this stage, and because TUNEL positive cells and BrdU positive cells were detected in both fibers and epithelial cells. Relative levels of β - and γ -crystallin were estimated from fluorescent intensity analysis as described (Madakashira et al., 2012)

SDS-PAGE and Western Blotting

Lenses were dissected from embryos and homogenized in RIPA buffer (50mM Tris HCl pH 8, 150mM NaCl, 1% NP40, 0.5% sodium deoxycholate) with protease inhibitor (Sigma-

Aldrich, St. Louis, MO, USA). Proteins were analyzed on 12% Tris-glycine gels and transferred to PVDF membrane. Membranes were incubated with PBST with 3% BSA, probed with primary antibodies (Akt 1:2000; phospho-Akt 1:1000; ERK1/2 1:2000; phospho-ERK1/2 1:1000; phospho-p53 1:1000; phosphoSer63/73-c-Jun 1:1000, Aquaporin0 1:2000, phospho-MDM2 1:1000) overnight at 4°C and then incubated with secondary antibody for 2hr at room temperature. The primary antibodies for phosphorylated AKT (Ser 473, 9101), phosphorylated ERK1/2 (Thr 202/Tyr 204, 9271) and phosphorylated MDM2 (Ser 166) were purchased from Cell Signaling Technology, Danvers, MA, USA. The primary antibodies for phosphorylated p53 (Ser 15, sc-101762) and phosphorylated c-JUN (Ser 63/Ser 73, sc-16312) and GAPDH (sc-25778) were obtained from Santa Cruz Biotechnology (Santa Cruz, CA, USA) and used as a dilution of 1:1000. The expression of GAPDH was used as the loading control. Binding of primary antibodies was detected using an anti-rabbit HRP-conjugated secondary antibody (A0545, Sigma-Aldrich) diluted at 1:5000, followed by using the Clarity Western ECL Substrate (Bio Rad Laboratories, Hercules, CA, USA) according to manufacturer instructions. Western blot images were acquired via radiographic film and the intensity of immunoreactivity was quantified by ImageJ software.

Quantitative RT-qPCR

The expression levels of selected genes were analyzed by RT-qPCR. Total RNA was extracted from the lenses using the Total RNA mini kit (IBI, Scientific, Peosta, IA, USA). cDNA was synthesized by reverse transcription using random primers and the superscript II reverse transcriptase (Invitrogen), according to the manufacturer's instructions. qPCR assays were performed on the cDNA using Gotaq Green Master Mix (Promega, Madison, WI, USA) following the manufacturer's instruction and read using CFX connect (Bio Rad Laboratories). Intron-spanning primers were designed to specifically quantify targeted mRNA transcripts (Supplementary table 1). Each biological sample was analyzed in triplicate by qPCR. The expression of GAPDH was used as an endogenous control. The cycling conditions consisted of 1 cycle at 95° C for 100s for denaturation, followed by 40 three-step cycles for amplification (each cycle consisted of 95° C incubation for 20s, an appropriate annealing temperature for 10s, and product elongation at 70° C incubation for 20s). The melting curve cycle was generated after PCR amplification. The reaction specificity was monitored by determination of the product melting temperature, and by checking for the presence of a single DNA band on agarose gels from the RT-qPCR products. Gene expression was calculated and normalized to *Gapdh* level using delta-delta Ct method (Applied Biosystems).

RESULTS

Balancing PTEN and FGFR2 in lens cell survival and proliferation

Loss of Pten restores lens size in FGFR2-deficient lenses—To generate the required mice, the *Le-Cre* transgene was used to delete loxP-flanked (floxed) alleles of *Fgfr2* (*Fgfr2*^{+/+}), *Pten* (*Pten*^{+/+}), or both *Fgfr2* and *Pten* (*Pten/R2*^{+/+}) in mouse lens precursor cells at approximately embryonic day 9.5 (E9.5) of development. Control mice consisted of animals lacking the *Le-Cre* transgene, while homozygous for floxed alleles of

Pten, *Fgfr2*, or both *Pten* and *Fgfr2*. Since the *Le-Cre* transgene independently affects eye development on some genetic backgrounds (Dora et al., 2014), our experiments controlled for phenotypes resulting solely from the *Le-Cre* transgene with hemizygous *Le-Cre* mice containing wild-type alleles of *Fgfr2* and *Pten*. Quantitative reverse transcription PCR (RT-qPCR) confirmed the deletion of the floxed alleles (Fig 1 A, B). Both *Fgfr2*^{-/-} and (*Pten/R2*)^{-/-} lenses contained very few *Fgfr2* transcripts at E15.5, and *Pten* deletion alone failed to alter the abundance of *Fgfr2* transcripts compared to that in the control lenses (Fig. 1 A). Likewise, (*Pten/R2*)^{-/-} and *Pten*^{-/-} lenses exhibited efficient deletion of the *Pten* transcript, but lenses lacking *Fgfr2* alone displayed an increased number of *Pten* transcripts compared to Cre negative lenses (Fig. 1 B).

The gross morphology of *Pten*^{-/-} lenses was virtually indistinguishable from that of *Le-Cre* negative control lenses at E12.5 (compare Fig. 2 B to A), E15.5 (compare Fig. 2 F to E), and E18.5 (compare Fig. 2 J to I). Moreover, *Pten*^{-/-} lenses failed to display a significant difference in lens section planar area at any stage examined (Fig. 2 M). In contrast, lenses depleted of FGFR2, displayed a drastic size reduction at E12.5 (compare Fig. 2 C to A). In addition to decreased size, the presumptive fiber cells in the posterior of E12.5 *Fgfr2*^{-/-} lenses exhibited dramatically reduced elongation toward the anterior epithelium (compare Fig. 2 C' to A' white arrows). Interestingly, *Fgfr2*-deficient lenses possessed a consistent tilt towards the nasal side of the head (Fig. 2 C' black arrow). By E15.5, the *Fgfr2*^{-/-} lenses remained significantly smaller than control lenses and contained vacuolated central fiber cells (compare Fig. 2 G to E, G' to E', M). By E18.5, *Fgfr2*^{-/-} lenses remained abnormally small compared to control, *Pten*^{-/-} or (*Pten/R2*)^{-/-} lenses (compare Fig. 2 K to I, J and L, M). Thus, lenses lacking *Fgfr2* failed to achieve normal size or morphology and lenses lacking *Pten* developed normally.

Although isolated *Pten* deletion failed to alter lens morphology or size, deletion of both *Pten* and *Fgfr2* significantly rescued the reduced size of *Fgfr2*^{-/-} lenses (compare Fig. 2 D, H, L to C, G, K; M). By E12.5, primary fiber cell elongation in (*Pten/R2*)^{-/-} lenses advanced well beyond *Fgfr2*^{-/-} lenses (compare Fig. 2 D' to C'). At E15.5, (*Pten/R2*)^{-/-} lenses were virtually indistinguishable from control lenses, in both size and morphology (compare Fig. 2 H and H' to E and E'). Like control lenses, E15.5 (*Pten/R2*)^{-/-} lenses contained a single layer of epithelial cells lining the anterior surface with differentiating fiber cells at the equator, or bow region, of the lens (compare Fig. 2 H' to E'). At E18.5, lenses lacking both PTEN and FGFR2 were almost the same size as control lenses (compare Fig. 2 L to I, M). Although deletion of *Pten* permitted FGFR2-deficient lenses to reach nearly normal size, normal eyelid closure failed to occur in either *Fgfr2*^{-/-} or (*Pten/R2*)^{-/-} mice (compare Fig. 2 dashed box of L and K to I).

Pten deletion restores cell survival in FGFR2-deficient lenses—The loss of *Fgfr2* leads to smaller lenses, primarily because of decreased lens cell survival (Garcia et al. 2005). TUNEL analysis made it possible to determine if *Pten* deletion rescues cell survival in lens cells lacking *Fgfr2*. As expected, lenses lacking FGFR2 exhibited a significant increase in TUNEL positive nuclei at E12.5, compared to control lenses (compare Fig. 3 C to A, I). At this stage, *Fgfr2*^{-/-} lenses contained apoptotic cells in both the anterior and posterior sides

of the lens (Fig. 3 C). At E15.5, *Fgfr2*^{-/-} lenses contained fewer TUNEL positive cells than E12.5 *Fgfr2*^{-/-} lenses (compare Fig. 3 G to C), but significantly more than E15.5 control lenses (compare Fig. 3 G to E). At this stage, the *Fgfr2*^{-/-} apoptotic nuclei were mainly restricted to the lens epithelium (Fig. 3G-white arrows), with the fiber cells remaining TUNEL negative. Although deleting *Pten* in isolation actually resulted in a slight increase in apoptosis as compared to control lenses at E12.5 (compare Fig. 3 B to A, I), the simultaneous deletion of both *Pten* and *Fgfr2* significantly increased cell survival relative to *Fgfr2*^{-/-} lenses both at E12.5 (compare Fig. 3 D to C, I) and at E15.5 (compare Fig. 3 H to G, J). TUNEL positive nuclei nearly disappeared in both control and *Pten*^{-/-} lenses by E15.5 (Fig. 3 F, J).

The effect of *Pten* deletion on lens cell proliferation—To determine if an increase in cellular proliferation contributed to the restoration of lens size in (*Pten/R2*)^{-/-} lenses, we labeled embryos with BrdU. Neither *Pten*^{-/-} nor (*Pten/R2*)^{-/-} lenses displayed a significant difference in BrdU incorporation, relative to the control lenses, at E12.5 (compare Fig. 4 B to A, D to A; I) or E15.5 (compare Fig. 4 F to E, H to E; J). Despite the unchanged proliferation index, several nuclei in the posterior (fiber cell compartment) of *Pten*^{-/-} and (*Pten/R2*)^{-/-} lenses ectopically incorporated BrdU (Fig. 4 B' and D'-white arrows). At E12.5, the *Fgfr2*^{-/-} lenses exhibited increased BrdU incorporation (compare Fig. 4 C to A, I), with an overall morphology reminiscent of a lens vesicle stage (E11) where primary fiber cells have not yet withdrawn from the cell cycle (Fig. 4C'-white arrows). The impaired elongation of primary fiber cells, in FGFR2-deficient lenses, made it difficult to discern epithelial cells from fiber cells. For this reason, we calculated the proliferation index for the whole lens, rather than for just lens epithelial cells, at E12.5 (Fig. 4C', I). By E15.5, BrdU positive cells only appeared in the epithelium of *Fgfr2*^{-/-} lenses. Therefore, at this stage, calculation of the proliferation index only accounted for epithelial cells (Fig. 4 G). By E15.5, *Fgfr2*^{-/-} lenses displayed no changes in epithelial cell proliferation compared to the Cre negative controls (compare Fig. 4 G to E, J). Neither *Pten* nor *Fgfr2* loss affected lens epithelial cell proliferation at E15.5 (Fig. 4 J) or E18.5 (Supp. Fig. 1 U). Taken together, the evidence suggests that *Pten* deletion restores FGFR2-deficient lens size primarily through increased cell survival rather than increased proliferation.

The impact of FGFR2 and PTEN on lens epithelial cell-to-fiber cell differentiation

Four hallmarks of fiber cell differentiation include: 1) cell cycle withdraw, 2) fiber cell elongation, 3) the onset of fiber cell structural protein expression, and 4) organelle loss. At E12.5, *Fgfr2*^{-/-} lenses exhibited defects in both fiber cell elongation (Fig. 2 C') and cell cycle withdrawal (Fig. 4 C, C'- white arrows). Although *Pten* deletion largely restored fiber cell elongation in the FGFR2-deficient lenses at E12.5 (compare Fig. 2 C' to D'), several posterior fiber cells failed to exit the cell cycle at this stage (Fig. 4D'-white arrows). Given the partial restoration of fiber cell differentiation in the FGFR2-deficient lenses by simultaneous deletion of *Pten*, we sought to determine more broadly which FGFR2-deficient lens phenotypes depended on the presence of PTEN.

The deletion of *Pten* partially restores reduced γ -crystallin expression in *Fgfr2*^{-/-} lenses

—The production of fiber cell-specific structural proteins represents

another hallmark of lens epithelial-to-fiber cell differentiation. Crystallin proteins make up the most abundant structural component of the mammalian lens fiber cells mass and permit lens transparency (reviewed in Harding and Dilley, 1976). Most β - and γ -crystallin proteins appear exclusively in lens fiber cells, with β -crystallin expression preceding the onset of γ -crystallin expression (reviewed in McAvoy et al., 1999). Both β - and γ -crystallin expression depend on FGFR signaling (Madakashira et al., 2012; Zhao et al., 2008). Moreover, ectopic activation of *Frs2a* in lens epithelial cells induces high levels of pAKT and pERK1/2 accompanied by the onset of β crystallin expression (Madakashira et al., 2012).

FGFR2-deficient lenses displayed dramatically reduced γ -crystallin (compare Fig. 5C to A), and modestly reduced of β -crystallin (compare Fig. 5K to I) expression at E12.5. As lens development progresses to E15.5 and E18.5, β - and γ -crystallin expression increased in *Fgfr2*^{-/-} lenses (Fig. 5O, G; Supp. Fig. 1 G, K). Additionally, the expression of *c-Maf*, a transcription factor known to regulate crystallin expression in the lens (Kim et al., 1999; Yang et al., 2006 et al. 2006), remained unaltered in *Fgfr2* deleted lenses at E15.5 (Fig. 5Q). Although *Pten* deletion alone failed to reduce β - or γ -crystallin expression, (compare Fig. 5J, N, B, F, to I, M, A, E) *Pten* deletion increased γ -crystallin expression in FGFR2-deficient lenses at E12.5 (compare Fig. 5D to C). As in E15.5 *Fgfr2*^{-/-} lenses, E15.5 (*Pten/R2*)^{-/-} lenses did not display a significant difference in *c-Maf* transcripts (Fig. 5Q).

Pten deletion fails to rescue reduced Aquaporin0 levels in FGFR2-deficient lenses

Aquaporin0, the most abundant lens fiber cell membrane protein, promotes fiber cell adhesion which minimizes extracellular space (Engel et al., 2008; Kumari et al., 2013). Deletion of *Frs2a* in the lens placode resulted in reduced Aquaporin0 expression (Madakashira et al., 2012). Likewise, *Fgfr2*^{-/-} lenses experienced significant reduction in Aquaporin0 protein, demonstrated by both immunofluorescence and western blot analysis (compare Fig. 6C to A, J, K). Aquaporin0 localizes to the fiber cell membranes and immunofluorescent analysis revealed that FGFR2-deficient fiber cells appear structurally different than Cre negative control lenses. Control and *Pten*^{-/-} lenses contain Aquaporin0 expression in columns extending the length of the lens fiber cell mass representing individual lens fiber cells (Fig. 6A and B). In contrast, *Fgfr2*^{-/-} lenses exhibited circular Aquaporin0 stained structures in the center of the lens. (compare Fig. 6 arrows in C to A). Like *Fgfr2*^{-/-} lens fiber cells, (*Pten/R2*)^{-/-} fiber cells displayed intense expression of Aquaporin0 in a circular pattern (Fig 6. D), and Aquaporin0 expression levels remained low (Fig. 6J, K). Therefore, deleting *Pten* failed to restore either the normal amount of Aquaporin0 protein or the normal structure of the central fiber cells in FGFR2 deficient lenses.

Fgfr2^{-/-} lens fiber cells experience nuclear retention and reduced Dnasell β expression in the presence or absence of Pten

Between E16 and E18, central lens fiber cells initiate the removal of cell nuclei, a process that requires the nuclease *Dnasell β* (Bassnett, 1997, 2009; Chaffee et al., 2014; Nakahara et al., 2007). Both *Fgfr2*^{-/-} and (*Pten/R2*)^{-/-} lenses retained nuclei in central lens fiber cells (Fig. 6G, and H). Thus, the absence of fiber cell denucleation represents another differentiation defect in FGFR2-deficient lenses that the simultaneous deletion of *Pten* failed to rescue. TUNEL analysis

reveals DNA breakdown that takes place normally as a consequence of fiber cell denucleation. At E18.5, both control and *Pten*^{-/-} lenses contained numerous TUNEL positive foci in the central fiber cell mass, the site of active denucleation (Fig. 6F and E-white arrows). In contrast, neither *Fgfr2*^{-/-} nor (*Pten/R2*)^{-/-} lenses exhibited abundant TUNEL positive staining in this region (Fig. 6G, H), although a few (*Pten/R2*)^{-/-} central fiber cells contained TUNEL positive foci (Fig. 6H-white arrow). Given the impairment of nuclear degradation in *Fgfr2*^{-/-} and (*Pten/R2*)^{-/-} lenses we examined the expression of *DnaseIIβ* by qRT-PCR. Both *Fgfr2*^{-/-} and (*Pten/R2*)^{-/-} lenses exhibited a significant reduction in *DnaseIIβ* transcripts (Fig. 6I). *Pten*^{-/-} lenses contained normal amounts of *DnaseIIβ* transcripts (Fig. 6I).

The deletion of *Pten* normalizes several downstream signaling pathways affected by *Fgfr2* loss in the lens

Pten deletion restores AKT and ERK1/2 activation in *Fgfr2*-deficient lenses—FGFR signaling and PTEN work antagonistically in terms of their impact on both PI3-K/AKT and MAPK/ERK1/2 (Di Cristofano and Pandolfi, 2000; Weng et al., 2001a; Weng et al., 2001b). The activation of AKT, by phosphorylation, promotes cell survival. In contrast, PTEN initiates apoptotic pathways, in part, by inhibiting AKT activation. The ERK1/2 sensitive cellular responses include the promotion of cellular proliferation, migration, and differentiation.

At E15.5, *Pten*^{-/-} lenses displayed over a 7-fold increase in p-AKT (Fig. 7A, B) relative to control lenses. Surprisingly, *Pten* deletion reduced the total level of AKT protein (Fig. 7A, C). *Pten*^{-/-} lenses also experienced a significant, albeit more modest (1.3-fold), increase in p-ERK1/2 relative to the increase in pAKT (Fig. 7A, compare differences between *Pten*^{-/-} lenses to control lenses in B and D). *Pten* deletion did not alter the total amount of ERK1/2 protein (Fig. 7E).

At E15.5, *Fgfr2*^{-/-} lenses exhibited a 28.8% reduction in p-AKT and a 26% reduction in p-ERK1/2 signal in comparison to control lenses (Fig. 7A, B, D). The (*Pten/R2*)^{-/-} lenses experienced nearly a 6-fold increase in p-AKT expression when compared to control lenses. However, (*Pten/R2*)^{-/-} lenses experienced the same quantitative increase in p-ERK1/2 as seen in the *Pten*^{-/-} lenses (Fig. 7D). The total level of ERK1/2 protein remained unchanged in (*Pten/R2*)^{-/-} lenses, but like single deletion of *Pten*, (*Pten/R2*)^{-/-} lenses had reduced levels of total AKT protein (Fig. 7A, C, E).

PTEN loss suppresses the increase in p53 and cJun phosphorylation in FGFR2-deficient lenses—Mechanistically, p53 lies at the heart of most apoptotic pathways. Although normally cells maintain low levels of p53, phosphorylation of p53 on Ser15 stabilizes the protein and promotes apoptosis. *Fgfr2* deletion increased the phosphorylation of Ser15 on p53 in the lens (Fig. 8A, B). Increased p-p53 levels in *Fgfr2*-deficient lenses accompany a dramatic decline in the level of phosphorylated MDM2, a negative regulator of p53 (Fig. 8A, D). However, while the loss of *Pten* alone had no significant effect on p53 Ser15 phosphorylation, *Pten* deletion in FGFR2-deficient lenses

reduced p53 phosphorylation to control levels (Fig. 8A, B) and largely restored the level of p-MDM2 (Fig 8A, D).

Phosphorylation of the c-Jun transcription factor can either activate or suppress apoptotic pathways depending on the cellular context. Phosphorylated (activated) c-Jun inhibits apoptosis by increasing the transcription of the AKT activator, *Pdk1*, while simultaneously inhibiting the transcription of both *p53* and *Pten* (reviewed in Dhanasekaran and Reddy, 2008; Kolomeichuk et al., 2008). Conversely, the apoptotic pathways activated by PTEN and p53 require phosphorylated c-Jun, as a component of AP-1, to promote the transcription of pro-apoptotic genes such as, *Bak1*, *Tnf* and *Fas* (reviewed in Dhanasekaran and Reddy, 2008). In addition to regulating apoptosis, c-Jun activation can initiate both cell proliferation and differentiation, and can act downstream of FGFR signaling (reviewed in Dhanasekaran and Reddy, 2008). FGFR2-deficient lenses up-regulate the phosphorylation of c-JUN (Fig. 8A, C). The deletion of *Pten* alone did not affect the phosphorylation of c-JUN, but *Pten* deletion restored c-JUN phosphorylation to normal levels in FGFR2-deficient lenses (Fig 8A, C).

DISCUSSION

A proper balance between PTEN and FGFR signaling is crucial in both the development and homeostatic maintenance of organs and tissues. Developmentally, the outcome of FGFR signaling is diverse, but includes enhanced proliferation, survival, and, in the case of the lens, promotes cell cycle withdraw and differentiation. Aberrant FGFR signaling can encourage tumorigenesis by driving proliferation, enhancing survival, and promoting angiogenesis (Turner and Grose, 2010). Conversely, PTEN antagonizes two of the major pathways stimulated by FGFR signaling (MAPK/ERK1/2 and PI3K/AKT) and plays an important role in inhibiting proliferation and stimulating apoptosis. In addition to its role as a tumor suppressor, PTEN participates in early developmental processes and morphogenesis. Embryonic survival requires PTEN; and tissue specific deletions in *Pten* demonstrate a loss of appropriate apoptosis during embryonic development (Di Cristofano et al., 1998; Li et al., 2002; Tiozzo et al., 2009).

As previously reported, the loss of FGFR2 in the lens placode resulted in both apoptosis and fiber cell differentiation defects (Garcia et al., 2005). However, in contrast to the deletion of both *Fgfr1* and *Fgfr2* in the lens placode (Garcia et al., 2011), or the deletion of *Fgfr1*, *Fgfr2* and *Fgfr3* in the lens vesicle (Zhao et al., 2008), many aspects of differentiation normalized subsequent to E12.5 (see Fig. 4, 5). In fact, the reduced β - and γ -crystallin expression (Fig. 5) and delay in fiber cell cycle withdrawal (Fig. 4) observed in *Fgfr2*^{-/-} lenses appears to represent a delay in development rather than a block in differentiation. The persistence of Pax6 expression in the posterior cells of the *Fgfr2*^{-/-} lens at E12.5 also disappears by E15.5, further supporting a lens developmental delay in this genotype (Supp. Fig. 2). An initial lens developmental delay in the absence of *Fgfr2* may be a consequence of the expression pattern of each *Fgfr* gene. The lens placode expresses both *Fgfr1* and *Fgfr2*, but *Fgfr3* expression only initiates as fiber cell differentiation commences between E11 and E12. By birth, *Fgfr3* is the most abundantly expressed *Fgfr* gene (Hoang et al., 2014). Therefore, the increasing

expression of *Fgfr3* may compensate for early developmental defects resulting from FGFR2 deficiency.

Despite the amelioration of many of the early differentiation deficits in FGFR2-deficient lenses, some differentiation defects persisted. These included reduced expression and abnormal patterning of Aquaporin0, reduced *DnaseII β* and a block in fiber cell denucleation. The persistence of these abnormalities in the *Fgfr2*^{-/-} lenses suggests that fiber cell denucleation, and the expression of Aquaporin0 and *DnaseII β* depend specifically on FGFR2, or that these features of differentiation exhibit particular sensitivity to the level of overall FGFR signaling. Alternatively, perhaps the early reduction of FGFR signaling creates a pattern of abnormalities that subsequent increases in *Fgfr3* expression fail to rescue.

To further understand the mechanistic role of FGFR2 in lens development, we examined the epistatic relationship of *Fgfr2* and *Pten* during lens development. Given the known suppression of AKT activation by PTEN, we anticipated that *Pten* deletion would restore lens cell survival to FGFR2-deficient lens cells. However, the ability of *Pten* deletion to rescue lens differentiation defects, resulting from *Fgfr2* deletion, remained difficult to predict. Ectopic over activation of FRS2 α in the lens promotes enhanced AKT and ERK1/2 activation followed by differentiation in central lens epithelial cells (Madakashira et al., 2012). The isolated deletion of *Pten* in the lens elevated pAKT and resulted in abnormal Na⁺/ATPase activity and cataracts without major disruptions in prenatal lens structure (Sellitto et al., 2013). Therefore, despite increased AKT activation, central lens epithelial cells fail to undergo ectopic fiber cell differentiation in the absence of PTEN. To date, no previous publications explored ERK activation in PTEN-deficient lenses.

The simultaneous deletion of *Pten* and *Fgfr2* at the lens placode stage, successfully decoupled the apoptotic phenotype from the differentiation phenotype associated with FGFR2-deficient lenses. The *Pten* deletion prevented the activation of apoptotic pathways that normally kill FGFR2-deficient lens cells. The deletion of *Pten*, in the presence or absence of *Fgfr2* increased AKT phosphorylation over 5-fold and AKT activation stimulates several survival pathways in cells. In addition to promoting cell survival, AKT inhibits apoptotic pathways. Activated AKT phosphorylates MDM2 on Ser166, Ser186 and Ser188. Phosphorylation at these three sites stabilizes MDM2 and increases the ability of MDM2 to destabilize p53, thereby inhibiting apoptosis (Levav-Cohen et al., 2014). Additionally, since p53 promotes the transcription of *Pten*, AKT phosphorylation of MDM2 increases AKT activation in a positive feedback loop in normal cells (Mayo et al., 2002; Mayo and Donner, 2002).

In *Fgfr2*^{-/-} lenses, phosphorylated AKT levels decline (Fig 7A, B), while the levels of p53 containing phosphorylation on Ser18 (the murine equivalent of Ser15) remain elevated (Fig. 8A, B). Dramatically decreased MDM2 phosphorylation in the *Fgfr2*-deficient lenses also provides an explanation for increased p-p53 levels (Fig 7A, D). Phosphorylation of Ser15/18 promotes the association of p53 with histone acetyltransferases required for p53-mediated transcriptional activation (Loughery et al., 2014), and these acetyltransferases also stabilize p53 by inhibiting p53 ubiquitination (Ito et al., 2002; Sakaguchi et al., 1998). Elevated

phosphorylation of Ser18 on p53 (p-p53) in the *Fgfr2*^{-/-} lenses explains the increased levels of *Pten* transcript in these lenses (Fig. 1B). However, deletion of *Pten*, or the simultaneous deletion of *Pten* and *Fgfr2*, in the lens, leads to AKT activation increased beyond the level of control lenses with a corresponding decline in p-p53 (Fig. 8A, B). Taken together, these data suggest that FGFR2 normally promotes cell survival in the lens by activating AKT, which reduces p-p53 levels and *Pten* transcription. *Pten* deletion also induced a small, but significant, increase in ERK phosphorylation in lenses, both in the presence and absence of *Fgfr2* (Fig. 7A, D). However, it remains a possibility that the dramatic rise in activated AKT, resulting from *Pten* deletion, rescues apoptosis in the *Fgfr2*-deficient lenses through a mechanism unrelated to *Fgfr2* loss. In addition, since *Fgfr2*-deletion results in increased *Pten* transcripts (Fig. 1B), decreased lens cell survival and differentiation defects might directly result from *Pten* overexpression rather than from loss of *Fgfr2*-signaling per se. The distinction of these possibilities will require further experimentation.

The JNK subfamily of MAP kinases also play a fundamental, yet complex role in cellular survival. The activation (phosphorylation) of c-JUN by JNKs can either enhance or inhibit cell survival dependent on the tissue type and apoptotic stimuli (Hettinger et al., 2007; Morishima et al., 2001; Resnick and Fennell, 2004). For example, in neuronal cells, serine to alanine mutations at the phosphorylation sites of *c-Jun* at positions 63 and 73, resulted in resistance to kainate-induced apoptosis, and the same mutations conferred resistance to UV light-induced apoptosis in fibroblasts (Behrens et al., 1999). In contrast, nutrient deprivation in fibroblasts lacking *c-Jun* induces robust apoptosis (Hettinger et al., 2007). In fact, in fibroblasts, and many cancer cell lines, c-JUN directly suppresses *Pten* transcription and enhances *Pdk1* transcription, both of which result in enhanced AKT activation and survival (Hettinger et al., 2007; Lopez-Bergami et al., 2010).

Lenses lacking *Fgfr2* experienced marked elevation in phosphorylated c-JUN, but the level of activated c-JUN returns nearly to baseline upon the additional deletion of *Pten* (Fig. 8A, C). Therefore, in contrast to fibroblasts, increased c-JUN phosphorylation in lenses lacking *Fgfr2* correlates with increased apoptosis (Fig. 3C, G, I, J) and increased *Pten* transcript levels (Fig 1B). In the absence of *Fgfr2*, PTEN signaling pushes lens cells toward apoptosis. *Pten* deletion restores homeostatic balance and survival in the FGFR2-deficient lenses.

Although *Pten* deletion rescues the apoptosis resulting from the loss of *Fgfr2* in the lens, normal, endogenous apoptosis during lens development proceeds without PTEN. Despite greater than 7-fold increase in p-AKT in *Pten*-deficient lenses, not all lens apoptosis depends on PTEN (Fig. 3I; Supp. Fig. 3 B, F). In fact, *Pten* deletion led to a roughly two-fold increase in lens apoptosis at E12.5, but this level of apoptosis may be an effect of the *Le-Cre* transgene (see discussion below). During normal lens morphogenesis, apoptosis occurs in the lens stalk, a transient structure connecting the lens vesicle to the overlying presumptive corneal epithelium. The lens stalk derives from the anterior edges of the lens pit and this area contains numerous apoptotic cells in both control (Supp. Fig. 2 A, E-white arrows) and *Pten*^{-/-} lenses (Fig. 3I; Supp. Fig. 3 B, F white arrows). The maintenance of endogenous apoptosis in the absence of *Pten* contrasts with that in involuting mammary glands and developing lung epithelial cells where PTEN-deficiency enhances cell survival and leads to tissue enlargement (Li et al., 2002; Tiozzo et al., 2009). Lens cells also

underwent normal DNA degradation related to nuclear removal during fiber cell differentiation in the absence of *Pten* (Fig. 6F).

Although elevated AKT, ERK1/2, and c-Jun activation commonly lead to increased proliferation, with the exception of elevated BrdU incorporation in *Fgfr2*^{-/-} lenses at E12.5, none of the lenses examined experienced alterations in epithelial cell proliferation. The increased proliferation seen in *Fgfr2*^{-/-} lenses at E12.5 may reflect a delay in cell cycle withdrawal rather than a primary proliferation increase. In any case, PTEN deficiency rescues the increase in proliferation seen in FGFR2-deficient lens cells at E12.5. Therefore, despite the increased p-AKT and p-ERK1/2 in *Pten*^{-/-} and (*Pten/R2*)^{-/-} lenses (Fig. 7A, B D) and increased c-JUN activation in *Fgfr2*^{-/-} lenses, cell proliferation remains largely unaffected.

The robust restoration of AKT activation and modest increase in ERK1/2 activation (beyond levels of control lenses) in PTEN-deficient lenses proved insufficient to completely restore fiber cell differentiation in the absence of FGFR2. Moreover, unlike the over-activation of FGFR signaling which promotes fiber cell differentiation in central lens epithelial cells (Lovicu and Overbeek, 1998; Madakashira et al., 2012; Robinson et al., 1998; Robinson et al., 1995), high levels of pAKT and pERK1/2 in the *Pten*^{-/-} lens epithelium failed to stimulate ectopic fiber cell differentiation in the central lens epithelium. Taken together, these results suggest that FGFR2 activation provides an essential signal for some aspects of differentiation that elevations of both pAKT and pERK1/2, in the *Pten*-deleted lenses, can't replace. These include the normal expression level and pattern of Aquaporin0, the expression of *DnaseIIβ*, and fiber cell denucleation. Although fiber cell denucleation requires DNASEIIβ, the reduction of *DnaseIIβ* expression in *Fgfr2*^{-/-} lenses is approximately the same as that seen in mice heterozygous for *DnaseIIβ* null mutations where fiber cell denucleation occurs normally. Therefore, additional aspects of fiber cell denucleation must be compromised in *Fgfr2*^{-/-} lenses.

During the course of these studies, a manuscript describing lens phenotypes in hemizygous *Le-Cre* mice without LoxP flanked alleles on some genetic backgrounds raised concerns about any studies utilizing this particular *Cre* transgene (Dora et al., 2014). We performed several additional analyses comparing *Le-Cre* hemizygous mice to wildtype controls to account for any phenotypes relating to Cre transgene expression in these animals. We did observe a consistent increase in apoptosis relative to wildtype controls in the *Le-Cre* hemizygotes. We believe that this increased apoptosis explains the elevation in apoptosis seen upon the deletion of *Pten* (Fig. 3I). For additional information on this point see the supplemental discussion and supplemental figures 4 and 5.

In conclusion, lens cell survival depends on a critical balance of FGFR and PTEN signaling. Increased apoptosis and decreased lens size in FGFR2-deficient lenses reversed in the absence of *Pten*. However, defects in Aquaporin0 and *DnaseIIβ* expression, as well as defective fiber cell denucleation in the FGFR2-deficient lenses persisted following *Pten* deletion. *Pten* deletion also failed to rescue normal eyelid closure in the *Fgfr2*-deleted ocular surface ectoderm, and this phenotype probably contributes to the rapid degeneration of the anterior segment in both *Fgfr2*^{-/-} and (*Pten/R2*)^{-/-} postnatal eyes (data not shown). The

deletion of Pten increased the activation of both AKT and ERK above the level of the wild type lens in the presence or absence of FGFR2. The lens joins a growing list of tissues in which FGFR and PTEN signaling clearly interact. Human genetic diseases including achondroplasia, craniosynostosis, thanatophoric dysplasia, and cancer result from abnormal FGFR signaling. Likewise, mutations in Pten can cause Cowden's Syndrome, Autism, and many types of cancer. Determining the precise nature of how these signaling pathways interact with each other may well result in novel treatments to restore intracellular balance when one or the other pathway goes awry.

Supplementary Material

Refer to Web version on PubMed Central for supplementary material.

Acknowledgments

We would like to thank both the Center for Bioinformatics and Functional Genomics and the Center for Advanced Microscopy and Imaging at Miami University for maintaining equipment and helping to prepare data presented in this manuscript. We would also like to thank Sara Q. Perkins for technical assistance and Adam S. LeFever and Julia E. Robinson for assistance with editing the manuscript. This work was supported by a grant from the National Eye Institute, EY012995.

References

- Ahmad I, Iwata T, Leung HY. Mechanisms of FGFR-mediated carcinogenesis. *Biochimica et biophysica acta*. 2012; 1823:850–860. [PubMed: 22273505]
- Ashery-Padan R, Marquardt T, Zhou X, Gruss P. Pax6 activity in the lens primordium is required for lens formation and for correct placement of a single retina in the eye. *Genes & development*. 2000; 14:2701–2711. [PubMed: 11069887]
- Bassnett S. Fiber cell denucleation in the primate lens. *Investigative ophthalmology & visual science*. 1997; 38:1678–1687. [PubMed: 9286256]
- Bassnett S. On the mechanism of organelle degradation in the vertebrate lens. *Experimental eye research*. 2009; 88:133–139. [PubMed: 18840431]
- Bassnett, S.; Beebe, DC. Lens Fiber Differentiation. In: Robinson, ML.; Lovicu, FJ., editors. *Development of the Ocular Lens*. Cambridge; 2004. p. 214-244.
- Behrens A, Sibilia M, Wagner EF. Amino-terminal phosphorylation of c-Jun regulates stress-induced apoptosis and cellular proliferation. *Nature genetics*. 1999; 21:326–329. [PubMed: 10080190]
- Carter EP, Fearon AE, Grose RP. Careless talk costs lives: fibroblast growth factor receptor signalling and the consequences of pathway malfunction. *Trends in cell biology*. 2015; 25:221–233. [PubMed: 25467007]
- Chaffee BR, Shang F, Chang ML, Clement TM, Eddy EM, Wagner BD, Nakahara M, Nagata S, Robinson ML, Taylor A. Nuclear removal during terminal lens fiber cell differentiation requires CDK1 activity: appropriating mitosis-related nuclear disassembly. *Development*. 2014; 141:3388–3398. [PubMed: 25139855]
- Chandrasekher G, Sailaja D. Alterations in lens protein tyrosine phosphorylation and phosphatidylinositol 3-kinase signaling during selenite cataract formation. *Current eye research*. 2004a; 28:135–144. [PubMed: 14972719]
- Chandrasekher G, Sailaja D. Phosphatidylinositol 3-kinase (PI-3K)/Akt but not PI-3K/p70 S6 kinase signaling mediates IGF-1-promoted lens epithelial cell survival. *Investigative ophthalmology & visual science*. 2004b; 45:3577–3588. [PubMed: 15452065]
- Chow RL, Roux GD, Roghani M, Palmer MA, Rifkin DB, Moscatelli DA, Lang RA. FGF suppresses apoptosis and induces differentiation of fibre cells in the mouse lens. *Development*. 1995; 121:4383–4393. [PubMed: 8575338]

- Chung JH, Eng C. Nuclear-cytoplasmic partitioning of phosphatase and tensin homologue deleted on chromosome 10 (PTEN) differentially regulates the cell cycle and apoptosis. *Cancer research*. 2005; 65:8096–8100. [PubMed: 16166282]
- Dhanasekaran DN, Reddy EP. JNK signaling in apoptosis. *Oncogene*. 2008; 27:6245–6251. [PubMed: 18931691]
- Di Cristofano A, Pandolfi PP. The multiple roles of PTEN in tumor suppression. *Cell*. 2000; 100:387–390. [PubMed: 10693755]
- Di Cristofano A, Pesce B, Cordon-Cardo C, Pandolfi PP. Pten is essential for embryonic development and tumour suppression. *Nature genetics*. 1998; 19:348–355. [PubMed: 9697695]
- Dora NJ, Collinson JM, Hill RE, West JD. Hemizygous Le-Cre transgenic mice have severe eye abnormalities on some genetic backgrounds in the absence of LoxP sites. *PLoS one*. 2014; 9:e109193. [PubMed: 25272013]
- Engel A, Fujiyoshi Y, Gonen T, Walz T. Junction-forming aquaporins. *Current opinion in structural biology*. 2008; 18:229–235. [PubMed: 18194855]
- Franke TF, Hornik CP, Segev L, Shostak GA, Sugimoto C. PI3K/Akt and apoptosis: size matters. *Oncogene*. 2003; 22:8983–8998. [PubMed: 14663477]
- Garcia CM, Huang J, Madakashira BP, Liu Y, Rajagopal R, Dattilo L, Robinson ML, Beebe DC. The function of FGF signaling in the lens placode. *Developmental biology*. 2011; 351:176–185. [PubMed: 21223962]
- Garcia CM, Yu K, Zhao H, Ashery-Padan R, Ornitz DM, Robinson ML, Beebe DC. Signaling through FGF receptor-2 is required for lens cell survival and for withdrawal from the cell cycle during lens fiber cell differentiation. *Developmental dynamics : an official publication of the American Association of Anatomists*. 2005; 233:516–527. [PubMed: 15778993]
- Guntur AR, Reinhold MI, Cuellar J Jr, Naski MC. Conditional ablation of Pten in osteoprogenitors stimulates FGF signaling. *Development*. 2011; 138:1433–1444. [PubMed: 21385768]
- Harding CV, Reddan JR, Unakar NJ, Bagchi M. The control of cell division in the ocular lens. *International review of cytology*. 1971; 31:215–300. [PubMed: 4945052]
- Harding JJ, Dilley KJ. Structural proteins of the mammalian lens: a review with emphasis on changes in development, aging and cataract. *Experimental eye research*. 1976; 22:1–73. [PubMed: 767125]
- Hertzler-Schaefer K, Mathew G, Somani AK, Tholpady S, Kadakia MP, Chen Y, Spandau DF, Zhang X. Pten loss induces autocrine FGF signaling to promote skin tumorigenesis. *Cell reports*. 2014; 6:818–826. [PubMed: 24582960]
- Hettinger K, Vikhanskaya F, Poh MK, Lee MK, de Belle I, Zhang JT, Reddy SA, Sabapathy K. c-Jun promotes cellular survival by suppression of PTEN. *Cell death and differentiation*. 2007; 14:218–229. [PubMed: 16676006]
- Hoang TV, Kumar PK, Sutharzan S, Tsonis PA, Liang C, Robinson ML. Comparative transcriptome analysis of epithelial and fiber cells in newborn mouse lenses with RNA sequencing. *Molecular vision*. 2014; 20:1491–1517. [PubMed: 25489224]
- Ito A, Kawaguchi Y, Lai CH, Kovacs JJ, Higashimoto Y, Appella E, Yao TP. MDM2-HDAC1-mediated deacetylation of p53 is required for its degradation. *The EMBO journal*. 2002; 21:6236–6245. [PubMed: 12426395]
- Iyengar L, Patkunanathan B, Lynch OT, McAvoy JW, Rasko JE, Lovicu FJ. Aqueous humour- and growth factor-induced lens cell proliferation is dependent on MAPK/ERK1/2 and Akt/PI3-K signalling. *Experimental eye research*. 2006; 83:667–678. [PubMed: 16684521]
- Katoh M, Nakagama H. FGF receptors: cancer biology and therapeutics. *Medicinal research reviews*. 2014; 34:280–300. [PubMed: 23696246]
- Kim JI, Li T, Ho IC, Grusby MJ, Glimcher LH. Requirement for the c-Maf transcription factor in crystallin gene regulation and lens development. *Proceedings of the National Academy of Sciences of the United States of America*. 1999; 96:3781–3785. [PubMed: 10097114]
- Kolomeichuk SN, Bene A, Upreti M, Dennis RA, Lyle CS, Rajasekaran M, Chambers TC. Induction of apoptosis by vinblastine via c-Jun autoamplification and p53-independent down-regulation of p21WAF1/CIP1. *Molecular pharmacology*. 2008; 73:128–136. [PubMed: 18094076]

- Kumari SS, Gandhi J, Mustehsan MH, Eren S, Varadaraj K. Functional characterization of an AQP0 missense mutation, R33C, that causes dominant congenital lens cataract, reveals impaired cell-to-cell adhesion. *Experimental eye research*. 2013; 116:371–385. [PubMed: 24120416]
- Le AC, Musil LS. FGF signaling in chick lens development. *Developmental biology*. 2001a; 233:394–411. [PubMed: 11336503]
- Le AC, Musil LS. A novel role for FGF and extracellular signal-regulated kinase in gap junction-mediated intercellular communication in the lens. *The Journal of cell biology*. 2001b; 154:197–216. [PubMed: 11449001]
- Lemmon MA, Schlessinger J. Cell signaling by receptor tyrosine kinases. *Cell*. 2010; 141:1117–1134. [PubMed: 20602996]
- Levav-Cohen Y, Goldberg Z, Tan KH, Alsheich-Bartok O, Zuckerman V, Haupt S, Haupt Y. The p53-Mdm2 loop: a critical juncture of stress response. *Sub-cellular biochemistry*. 2014; 85:161–186. [PubMed: 25201194]
- Li L, Liu F, Salmonsens RA, Turner TK, Litofsky NS, Di Cristofano A, Pandolfi PP, Jones SN, Recht LD, Ross AH. PTEN in neural precursor cells: regulation of migration, apoptosis, and proliferation. *Molecular and cellular neurosciences*. 2002; 20:21–29. [PubMed: 12056837]
- Lopez-Bergami P, Kim H, Dewing A, Goydos J, Aaronson S, Ronai Z. c-Jun regulates phosphoinositide-dependent kinase 1 transcription: implication for Akt and protein kinase C activities and melanoma tumorigenesis. *The Journal of biological chemistry*. 2010; 285:903–913. [PubMed: 19910471]
- Loughery J, Cox M, Smith LM, Meek DW. Critical role for p53-serine 15 phosphorylation in stimulating transactivation at p53-responsive promoters. *Nucleic acids research*. 2014; 42:7666–7680. [PubMed: 24928858]
- Lovicu FJ, McAvoy JW. FGF-induced lens cell proliferation and differentiation is dependent on MAPK (ERK1/2) signalling. *Development*. 2001; 128:5075–5084. [PubMed: 11748143]
- Lovicu FJ, Overbeek PA. Overlapping effects of different members of the FGF family on lens fiber differentiation in transgenic mice. *Development*. 1998; 125:3365–3377. [PubMed: 9693140]
- Madakashira BP, Kobriniski DA, Hancher AD, Arneman EC, Wagner BD, Wang F, Shin H, Lovicu FJ, Reneker LW, Robinson ML. Frs2alpha enhances fibroblast growth factor-mediated survival and differentiation in lens development. *Development*. 2012; 139:4601–4612. [PubMed: 23136392]
- Mayo LD, Dixon JE, Durden DL, Tonks NK, Donner DB. PTEN protects p53 from Mdm2 and sensitizes cancer cells to chemotherapy. *The Journal of biological chemistry*. 2002; 277:5484–5489. [PubMed: 11729185]
- Mayo LD, Donner DB. The PTEN, Mdm2, p53 tumor suppressor-oncoprotein network. *Trends in biochemical sciences*. 2002; 27:462–467. [PubMed: 12217521]
- McAvoy JW. Cell division, cell elongation and the co-ordination of crystallin gene expression during lens morphogenesis in the rat. *Journal of embryology and experimental morphology*. 1978; 45:271–281. [PubMed: 353215]
- McAvoy JW, Chamberlain CG, de Iongh RU, Hales AM, Lovicu FJ. Lens development. *Eye*. 1999; 13(Pt 3b):425–437. [PubMed: 10627820]
- Mester J, Eng C. When overgrowth bumps into cancer: the PTEN-opathies. *American journal of medical genetics Part C, Seminars in medical genetics*. 2013; 163C:114–121.
- Morishima Y, Gotoh Y, Zieg J, Barrett T, Takano H, Flavell R, Davis RJ, Shirasaki Y, Greenberg ME. Beta-amyloid induces neuronal apoptosis via a mechanism that involves the c-Jun N-terminal kinase pathway and the induction of Fas ligand. *The Journal of neuroscience : the official journal of the Society for Neuroscience*. 2001; 21:7551–7560. [PubMed: 11567045]
- Nakahara M, Nagasaka A, Koike M, Uchida K, Kawane K, Uchiyama Y, Nagata S. Degradation of nuclear DNA by DNase II-like acid DNase in cortical fiber cells of mouse eye lens. *FEBS J*. 2007; 274:3055–3064. [PubMed: 17509075]
- Qu X, Hertzler K, Pan Y, Grobe K, Robinson ML, Zhang X. Genetic epistasis between heparan sulfate and FGF-Ras signaling controls lens development. *Developmental biology*. 2011; 355:12–20. [PubMed: 21536023]
- Resnick L, Fennell M. Targeting JNK3 for the treatment of neurodegenerative disorders. *Drug discovery today*. 2004; 9:932–939. [PubMed: 15501728]

- Robinson ML. An essential role for FGF receptor signaling in lens development. *Seminars in cell & developmental biology*. 2006; 17:726–740. [PubMed: 17116415]
- Robinson, ML. From Zygote to Lens: Emergence of the Lens Epithelium. In: Saika, S.; Werner, L.; Lovicu, FJ., editors. *Lens Epithelium and Posterior Capsular Opacification*. Springer; 2014. p. 3-17.
- Robinson ML, Ohtaka-Maruyama C, Chan CC, Jamieson S, Dickson C, Overbeek PA, Chepelinsky AB. Disregulation of ocular morphogenesis by lens-specific expression of FGF-3/int-2 in transgenic mice. *Developmental biology*. 1998; 198:13–31. [PubMed: 9640329]
- Robinson ML, Overbeek PA, Verran DJ, Grizzle WE, Stockard CR, Friesel R, Maciag T, Thompson JA. Extracellular FGF-1 acts as a lens differentiation factor in transgenic mice. *Development*. 1995; 121:505–514. [PubMed: 7539358]
- Sakaguchi K, Herrera JE, Saito S, Miki T, Bustin M, Vassilev A, Anderson CW, Appella E. DNA damage activates p53 through a phosphorylation-acetylation cascade. *Genes & development*. 1998; 12:2831–2841. [PubMed: 9744860]
- Sarbassov DD, Guertin DA, Ali SM, Sabatini DM. Phosphorylation and regulation of Akt/PKB by the rictor-mTOR complex. *Science*. 2005; 307:1098–1101. [PubMed: 15718470]
- Sellitto C, Li L, Gao J, Robinson ML, Lin RZ, Mathias RT, White TW. AKT activation promotes PTEN hamartoma tumor syndrome-associated cataract development. *The Journal of clinical investigation*. 2013; 123:5401–5409. [PubMed: 24270425]
- Stolen CM, Griep AE. Disruption of lens fiber cell differentiation and survival at multiple stages by region-specific expression of truncated FGF receptors. *Developmental biology*. 2000; 217:205–220. [PubMed: 10625547]
- Teven CM, Farina EM, Rivas J, Reid RR. Fibroblast growth factor (FGF) signaling in development and skeletal diseases. *Genes & Diseases*. 2014; 1:199–213. [PubMed: 25679016]
- Tiozzo C, De Langhe S, Yu M, Londhe VA, Carraro G, Li M, Li C, Xing Y, Anderson S, Borok Z, Bellusci S, Minoo P. Deletion of Pten expands lung epithelial progenitor pools and confers resistance to airway injury. *American journal of respiratory and critical care medicine*. 2009; 180:701–712. [PubMed: 19574443]
- Trimboli AJ, Cantemir-Stone CZ, Li F, Wallace JA, Merchant A, Creasap N, Thompson JC, Caserta E, Wang H, Chong JL, Naidu S, Wei G, Sharma SM, Stephens JA, Fernandez SA, Gurcan MN, Weinstein MB, Barsky SH, Yee L, Rosol TJ, Stromberg PC, Robinson ML, Pepin F, Hallett M, Park M, Ostrowski MC, Leone G. Pten in stromal fibroblasts suppresses mammary epithelial tumours. *Nature*. 2009; 461:1084–1091. [PubMed: 19847259]
- Turner N, Grose R. Fibroblast growth factor signalling: from development to cancer. *Nature reviews Cancer*. 2010; 10:116–129. [PubMed: 20094046]
- Wang Q, Stump R, McAvoy JW, Lovicu FJ. MAPK/ERK1/2 and PI3-kinase signalling pathways are required for vitreous-induced lens fibre cell differentiation. *Experimental eye research*. 2009; 88:293–306. [PubMed: 18938158]
- Weber GF, Menko AS. Phosphatidylinositol 3-kinase is necessary for lens fiber cell differentiation and survival. *Investigative ophthalmology & visual science*. 2006; 47:4490–4499. [PubMed: 17003444]
- Weng L, Brown J, Eng C. PTEN induces apoptosis and cell cycle arrest through phosphoinositol-3-kinase/Akt-dependent and -independent pathways. *Human molecular genetics*. 2001a; 10:237–242. [PubMed: 11159942]
- Weng LP, Smith WM, Brown JL, Eng C. PTEN inhibits insulin-stimulated MEK/MAPK activation and cell growth by blocking IRS-1 phosphorylation and IRS-1/Grb-2/Sos complex formation in a breast cancer model. *Human molecular genetics*. 2001b; 10:605–616. [PubMed: 11230180]
- Wesche J, Haglund K, Haugsten EM. Fibroblast growth factors and their receptors in cancer. *The Biochemical journal*. 2011; 437:199–213. [PubMed: 21711248]
- Wormstone IM, Wride MA. The ocular lens: a classic model for development, physiology and disease. *Philosophical transactions of the Royal Society of London Series B, Biological sciences*. 2011; 366:1190–1192. [PubMed: 21402579]
- Yang Y, Stopka T, Golestaneh N, Wang Y, Wu K, Li A, Chauhan BK, Gao CY, Cveklova K, Duncan MK, Pestell RG, Chepelinsky AB, Skoultschi AI, Cvekl A. Regulation of alphaA-crystallin via

Pax6, c-Maf, CREB and a broad domain of lens-specific chromatin. *The EMBO journal*. 2006; 25:2107–2118. [PubMed: 16675956]

Yu K, Xu J, Liu Z, Sosis D, Shao J, Olson EN, Towler DA, Ornitz DM. Conditional inactivation of FGF receptor 2 reveals an essential role for FGF signaling in the regulation of osteoblast function and bone growth. *Development*. 2003; 130:3063–3074. [PubMed: 12756187]

Zhang X, Tang N, Hadden TJ, Rishi AK. Akt, FoxO and regulation of apoptosis. *Biochimica et biophysica acta*. 2011; 1813:1978–1986. [PubMed: 21440011]

Zhao H, Yang T, Madakashira BP, Thiels CA, Bechtle CA, Garcia CM, Zhang H, Yu K, Ornitz DM, Beebe DC, Robinson ML. Fibroblast growth factor receptor signaling is essential for lens fiber cell differentiation. *Developmental biology*. 2008; 318:276–288. [PubMed: 18455718]

- Apoptosis caused by *Fgfr2*-deletion in the lens is rescued by *Pten*-deletion
- Deletion of *Pten* increases both AKT and ERK activation in the lens
- Lens differentiation defects caused by *Fgfr2* loss persist in the absence of *Pten*.

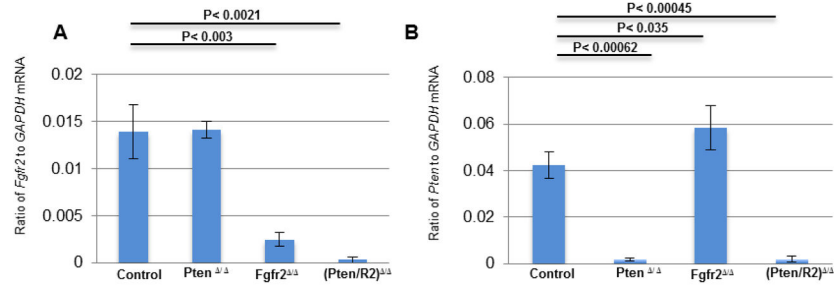


Figure 1. *Le-Cre* efficiently deletes LoxP-flanked *Pten* and *Fgfr2*

RT-qPCR was used to detect *Fgfr2* (A) and *Pten* (B) expression in E15.5 *Le-Cre* negative (Control), *Pten*^{-/-} *Fgfr2*^{-/-}, and (*Pten/R2*)^{-/-} lenses to determine the efficiency of the deletion of LoxP-flanked alleles. Lenses with LoxP-flanked *Pten* and the *Le-Cre* transgene (*Pten*^{-/-}) displayed similar expression levels of *Fgfr2* transcript as control lenses, but expressed very little *Pten* transcript. LoxP-Flanked *Fgfr2* lenses containing the *Le-Cre* transgene (*Fgfr2*^{-/-}) displayed a significant reduction in *Fgfr2* transcripts and a significant increase in *Pten* transcripts. Lenses containing both LoxP -flanked *Pten* and *Fgfr2* and the *Le-Cre* transgene (*Pten/R2*)^{-/-} contained almost no *Fgfr2* or *Pten* transcripts. Error bars represent standard error of the mean (s.e.m.) with significance level indicated above the relevant bars.

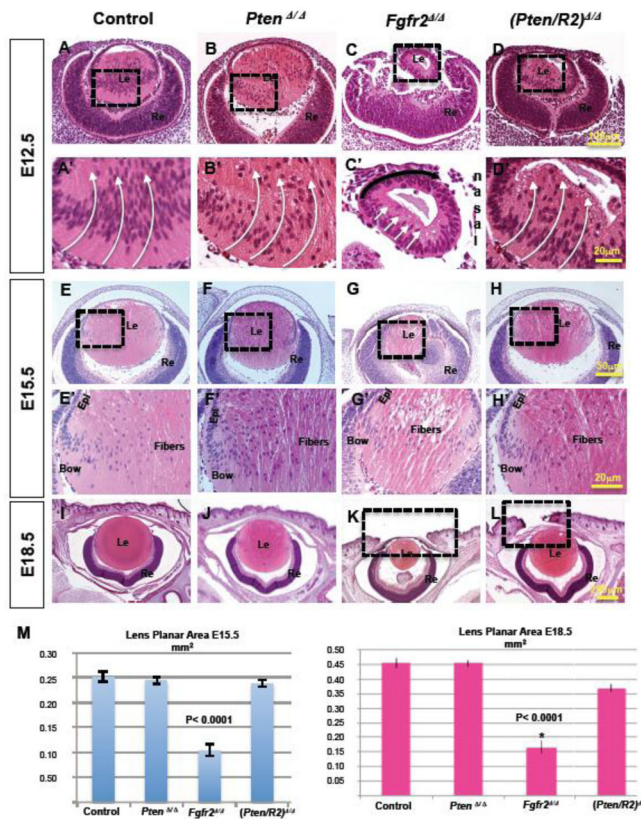


Figure 2. *Pten* deletion rescues the lens size and elongation defects in *Fgfr2*^{-/-} lenses
Hematoxylin and Eosin staining was implemented to analyze the morphology and size of the four different genotypes being compared, Cre-negative controls (A, A', E, E', I); *Pten*^{-/-} (B, B', F, F' J); *Fgfr2*^{-/-} (C, C', G, G' K); and *(Pten/R2)*^{-/-} (D, D', H, H' L) at E12.5 (A–D, A'–D'), E15.5 (E–H, E'–H'), and E18.5 (I–L). A'–D' and E'–H' are higher magnifications of the boxed in regions of A–D and E–H respectively. Lens planar area measurements in mm² were taken using a Nikon TI-80 microscope in conjunction with their advanced research software at E15.5 and E18.5 (M). At E12.5 the posterior cells of *Fgfr2*^{-/-} lenses did not elongate (compare C to A, C' to A'-white arrows). Deleting *Pten* restored the fiber cell elongation phenotype displayed in FGFR2-deficient lenses (compare D to C, D' to C'-white arrows). At E15.5 and E18.5 *Fgfr2*^{-/-} lenses were significantly smaller than control lenses (compare G to E, K to I, M). *Pten* deletion rescued lens size in FGFR2-deficient lenses at E15.5 and E18.5 (compare H to G, L to K), but did not restore the eyelid closure phenotype present in FGFR2-deficient lenses (compare boxed regions in L and K to I). *Pten* deletion, by itself, did not visibly alter the size or morphology of the lens at any of the 3 stages compared (compare B, B', F, F' J to A, A' E, E', I, M). Errors bars on the graphs represent s.e.m, with each bar representing a minimum of 9 measurements (3 sections from the lens center of 3 different embryos). Scale bars: 100μm in AD; 20 μm in A'–D' and E'–H'; 50 μm in E'H; 200 μm in (I–L).

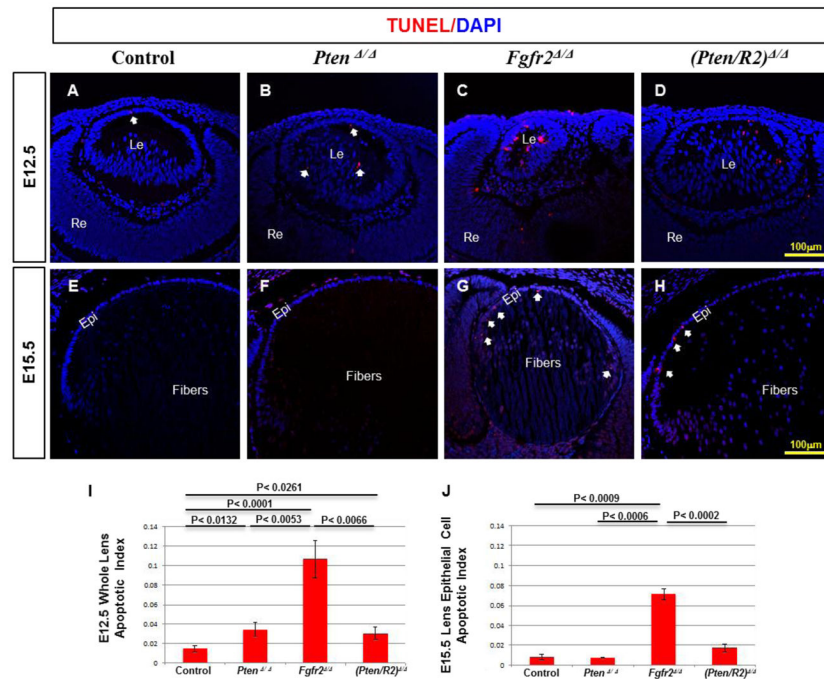


Figure 3. *Pten* deletion restores lens cell survival in FGFR2-deficient lenses

TUNEL analysis was implemented on E12.5 (A–D) and E15.5 (E–H) lenses comparing Cre-negative controls (A, E), *Pten*^{Δ/Δ} (B, F), *Fgfr2*^{Δ/Δ} (C, G), and *(Pten/R2)*^{Δ/Δ} (D, H). I and J represent the apoptotic index at E12.5 and E15.5, respectively. At E12.5, the apoptotic index was calculated for the entire lens due to the apoptosis detected in both posterior and anterior lens cells, whereas the apoptotic index was only calculated for the epithelial cell layer at E15.5 as apoptosis was only detected in the epithelium. At E12.5 and E15.5 *Fgfr2*^{Δ/Δ} lenses displayed a significant increase in TUNEL positive cells as compared to control lenses (compare C to A, G to E, I), although the apoptotic index was higher at E12.5 than E15.5 (compare C to G). At both E12.5 and E15.5 deleting *Pten* rescued the cell survival phenotype associated with FGFR2 loss (compare D to C, H to G, I, J). Despite the rescue of apoptosis when *Fgfr2*^{Δ/Δ} lenses are compared to *(Pten/R2)*^{Δ/Δ} lenses, *(Pten/R2)*^{Δ/Δ} lenses continued to exhibit higher levels of apoptosis at E12.5 and E15.5 (compare D to A, H to E, I, J). Moreover, the apoptotic index in *Pten*^{Δ/Δ} lenses was increased at E12.5 in comparison to control lenses (compare B to A-white arrows; I). Errors bars on the graphs represent s.e.m, with each bar representing a minimum of 9 measurements (3 sections from the lens center of 3 different embryos). Scale bars: 100μm in AH. White arrows point to TUNEL positive foci.

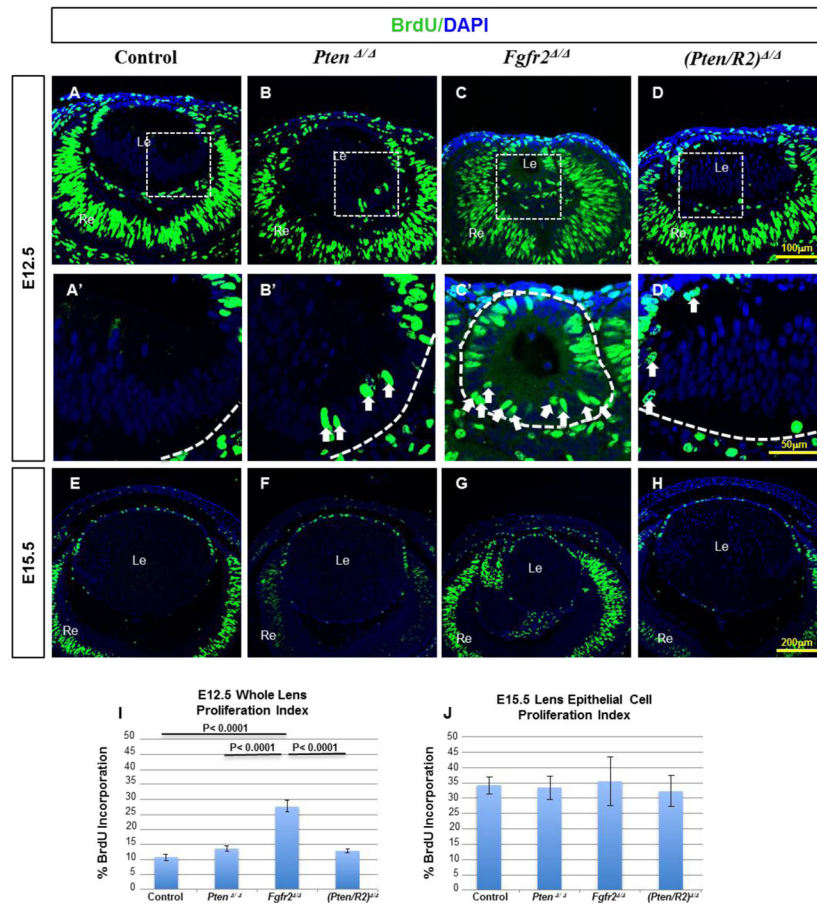


Figure 4. Cell cycle analysis in *Pten*^{-/-}, *Fgfr2*^{-/-}, and *(Pten/R2)*^{-/-} lenses

BrdU incorporation assay was used on Cre-negative controls (A, A', E), *Pten*^{-/-} (B, B', F), *Fgfr2*^{-/-} (C, C', G), and *(Pten/R2)*^{-/-} (D, D', H) to assess the impact of deleting *Pten*, *Fgfr2*, and the combination of the two on lens epithelial cell proliferation and cell cycle withdrawal. By E12.5, control lenses failed to exhibit any BrdU incorporation in the differentiating fiber cells (A, A'). E12.5 *Pten*^{-/-} (B, B'), *Fgfr2*^{-/-} (C, C'), and *(Pten/R2)*^{-/-} (D, D') lenses displayed BrdU incorporation of nuclei in the fiber cell mass, although *Fgfr2*^{-/-} lenses contained the most proliferation in posterior lens cells (compare C' to B' and D'). Furthermore, overall proliferation was increased in E12.5 *Fgfr2*^{-/-} lenses, yet was not significantly increased in *Pten*^{-/-} or *(Pten/R2)*^{-/-} lenses at this stage (I). By E15.5 (E–H, J) lens epithelial proliferation was not altered in *Pten*^{-/-} (F, J), *Fgfr2*^{-/-} (G, J), or *(Pten/R2)*^{-/-} (H, J). A'–D' represent boxed regions of A–D selected for higher magnification. Dashed white lines outline the edges of the lens and white arrows point towards posterior lens cells remaining proliferic (A'–D'). Errors bars on the graphs represent s.e.m, with each bar representing a minimum of 9 measurements (3 sections from the lens center of 3 different embryos). Scale bars: 100 μ m in A–D; 50 μ m in A'–D'; 200 μ m in E–H.

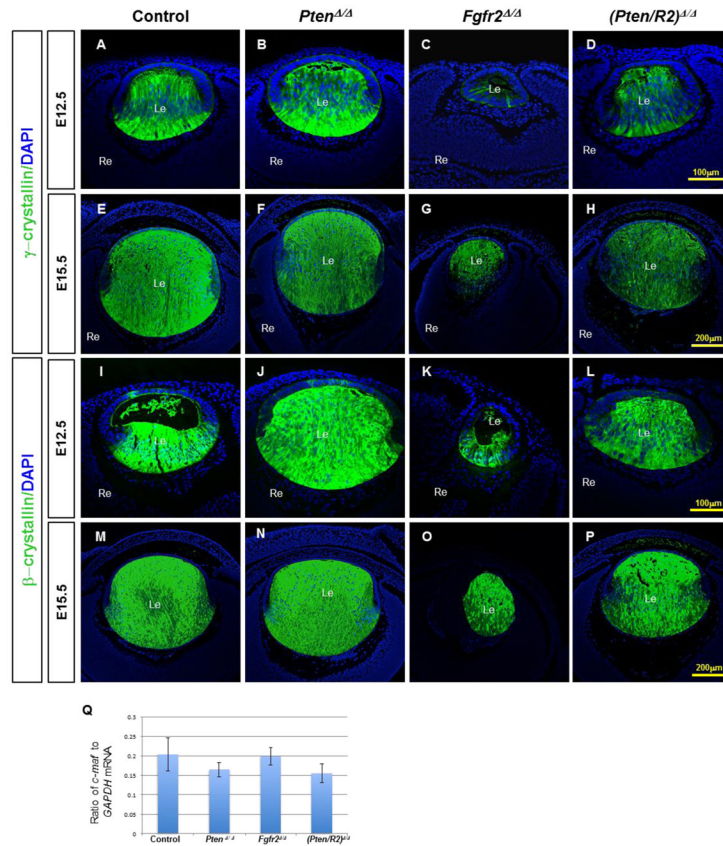


Figure 5. *Pten* deletion restores decreased β - and γ -crystallin expression to the FGFR2- deficient lenses at E12.5

Cre-negative control (A, E, I, M), *Pten*^{Δ/Δ} (B, F, J, N), *Fgfr2*^{Δ/Δ} (C, G, K, O), and *(Pten/R2)*^{Δ/Δ} (D, H, L, P) lenses were analyzed by immunohistochemistry at E12.5 (A–D, I–L), and E15.5 (E–H, M–P), to determine the expression of γ -crystallin (A–H) and β -crystallin (I–P). At E12.5 γ -crystallin was present in very few posterior cells of *Fgfr2*^{Δ/Δ} lenses (compare C to A). E12.5 *(Pten/R2)*^{Δ/Δ} lenses displayed an increase in γ -crystallin expression relative to *Fgfr2*^{Δ/Δ} lenses (compare D to C), but remained reduced in comparison to control lenses (compare D to A). By E15.5, *Fgfr2*^{Δ/Δ} lenses expressed γ -crystallin protein in all fiber cells (compare G to C). *c-Maf* transcript levels were not reduced in either *Fgfr2*^{Δ/Δ} or *(Pten/R2)*^{Δ/Δ} lenses (Q). Isolated *Pten* deletion did not alter γ -crystallin protein at E12.5 (compare B to A), or E15.5 (compare F to E). The quantification of *c-Maf* (Q) was standardized to *Gapdh* mRNA. Errors bars on the graphs represent s.e.m, with each bar representing a minimum of 9 measurements (3 sections from the lens center of 3 different embryos). Scale bars: 100 μ m in A–D, I–L; 200 μ m in E–H, M–P.

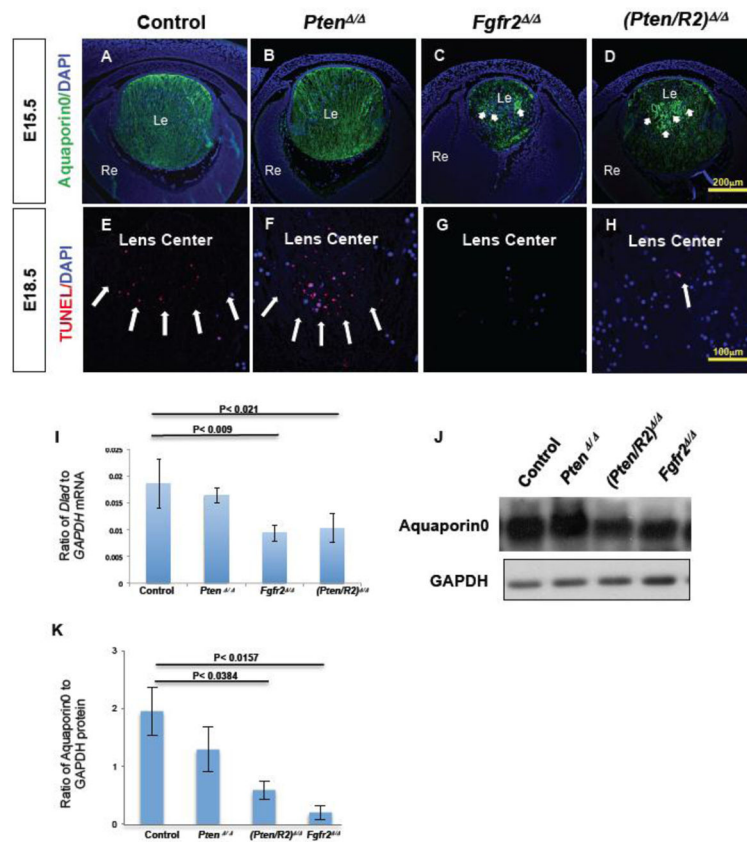


Figure 6. *Fgfr2*^{-/-} lenses exhibit reduced Aquaporin0 expression and a nuclear retention phenotype that *Pten* deletion fails to rescue. Cre-negative control (A, E), *Pten*^{-/-} (B, F), *Fgfr2*^{-/-} (C, G), and (*Pten/R2*)^{-/-} (D, H) lenses were analyzed for Aquaporin0 protein expression at E15.5 (A–D), and for denucleation by TUNEL at E18.5 (E–H). Both *Fgfr2*^{-/-} (compare C to A; J, K) and (*Pten/R2*)^{-/-} (Compare D to A; J, K) lenses experienced a reduced Aquaporin0 expression level. Additionally, *Fgfr2*^{-/-} (C) and (*Pten/R2*)^{-/-} (D) contained several heightened areas of Aquaporin0 expression in a circular pattern (C and D white arrows). Aquaporin0 expression in *Pten*^{-/-} lenses did not differ from controls (compare B to A; J, K). Western blot analysis was performed at E15.5 to confirm the reduced Aquaporin0 protein observed with FGFR2 deficiency (K). The western blot quantification was standardized to GAPDH protein. TUNEL analysis detected normal fiber cell DNA degradation in both control (E) and *Pten* deleted lenses (F). However DNA degradation in the central fiber cells was markedly reduced in both *Fgfr2*^{-/-} (G) and (*Pten/R2*)^{-/-} (H) lenses. Quantitative RT-PCR revealed a reduction in transcripts for *DnaseIIβ* at E16.5 (I). The quantification of *DnaseIIβ* was standardized to *GADPH* mRNA. Reduced transcript levels of *DnaseIIβ* were observed in *Fgfr2*^{-/-} and (*Pten/R2*)^{-/-} lenses (I). *Pten*^{-/-} lenses did not display defects in Aquaporin0 protein expression (J)/localization (B), nuclear removal (F), or *DnaseIIβ* expression (I). White arrows point towards heightened and abnormal expression of Aquaporin0 in C and D, and TUNEL foci in E, F, and H. Errors bars on the graphs represent s.e.m, with each bar representing a minimum of 9 measurements (3 sections from the lens center of 3 different embryos). Scale bars: 200 μm in A–D; 100 μm in E–H.

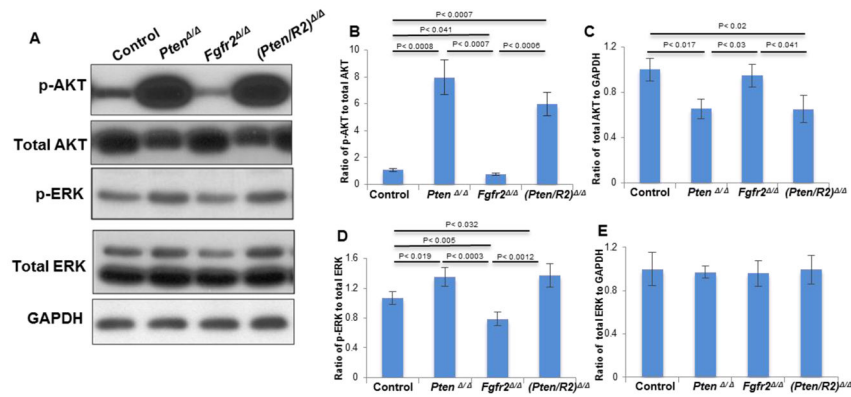


Figure 7. Deleting *Pten* restores pAKT and pERK1/2 in FGFR2-deficient lenses

E15.5 Cre-negative control, *Pten*^{-/-}, *Fgfr2*^{-/-}, and (*Pten/R2*)^{-/-} lenses were analyzed by western blot analysis to determine the impact of deleting *Pten*, *Fgfr2*, or both *Pten* and *Fgfr2* on activation of ERK1/2 and AKT. Levels of pAKT were significantly reduced in *Fgfr2*^{-/-} lenses (A, B). Additionally deleting *Pten* with the *Fgfr2* deletion raised the level of pAKT well beyond the levels of control lenses (A, B). As expected, *Pten*^{-/-} lenses experienced very high levels of pAKT (A, B). Interestingly, the total amount of AKT was reduced in both *Pten*^{-/-} lenses and (*Pten/R2*)^{-/-} lenses (A, C). *Fgfr2*^{-/-} lenses experienced a significant reduction in p-ERK (A, D), and additionally deleting *Pten* raised the level of pERK1/2 above that of control lenses (A, D). *Pten*^{-/-} lenses experienced modestly elevated levels of pERK1/2 (A, D). Total ERK levels remained unaltered in all of the examined genotypes (A, E). Total ERK1/2 and AKT were standardized to GAPDH while pERK1/2 and pAKT were normalized to total ERK1/2 and total AKT, respectively. Errors bars on the graphs represent s.e.m, with significance levels indicated above the relevant genotypes.

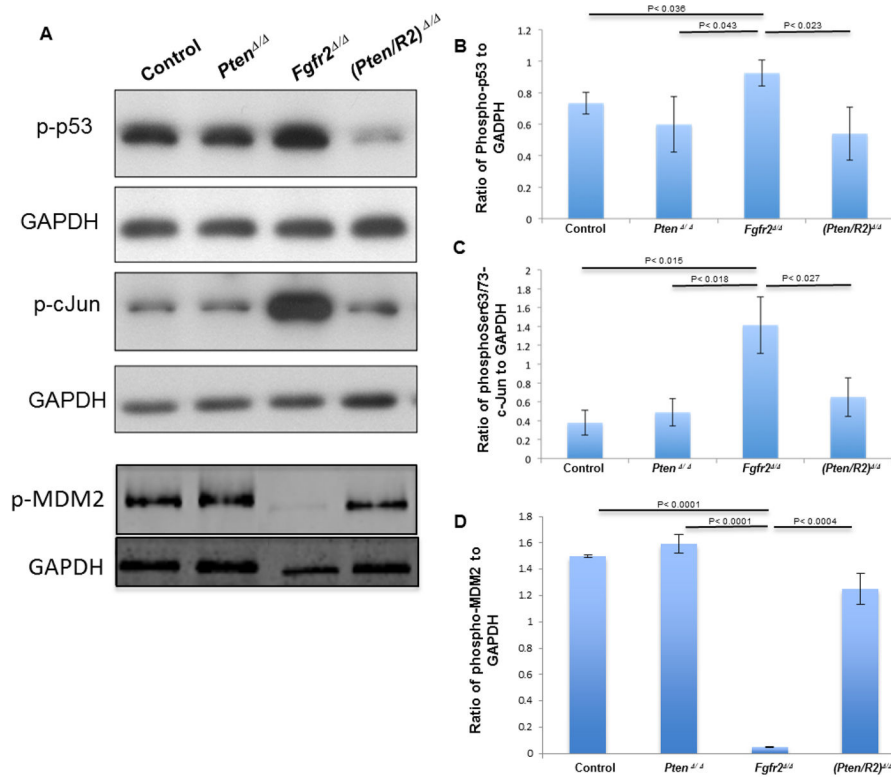


Figure 8. FGFR2 deficiency leads to increased activation of C-JUN and p53 and loss of MDM2 phosphorylation

E15.5 whole lenses of Cre-negative control, *Pten*^{-/-}, *Fgfr2*^{-/-}, and (*Pten/R2*)^{-/-} were analyzed by western blot analysis using antibodies to p-p53 (Ser 15), p-cJUN (Thr 63/Thr 73) and p-MDM2 (Ser 166). GAPDH was used as a loading control. *Fgfr2*^{-/-} lenses increased both phospho-p53 (A-top panel, B) and p-cJUN (A-3rd panel, C) while decreasing the amount of p-MDM2 (A-5th panel, D). The deletion of *Pten* lowered p-p53 in FGFR2-deficient lenses. Likewise deleting *Pten* returned cJUN activation and p-MDM2 to control levels (A-3rd panel, C and A-5th panel, D, respectively). Error bars on the graphs represent +/- s.e.m. p-p53, p-cJUN and p-MDM2 were standardized to GAPDH for quantification.